Acta metall. Vol. 31, No. 7, pp. 1079–1088, 1983
Printed in Great Britain.

0001-6160/83 $03.00 + .00

CONSTITUTIVE BEHAVIOR AND CRACK TIP FIELDS FOR MATERIALS UNDERGOING CREEP-CONSTRAINED GRAIN BOUNDARY CAVITATION

J. W. HUTCHINSON
Division of Applied Sciences, Harvard University, Cambridge, MA 02138, U.S.A.

(*Received* 13 *December* 1982)

Abstract—Based on micro-mechanical considerations, a phenomenological constitutive law is proposed for the steady creep of polycrystalline materials undergoing creep-constrained grain boundary cavitation. Singular stress and strain-rate fields at the tip of a stationary, plane strain crack are obtained revealing the role of cavitation on near-tip behavior.

Résumé—Nous proposons une loi phénoménologique constitutive, reposant sur des considérations micro-mécaniques, pour le fluage stationnaire de matériaux polycristallins présentant une cavitation intergranulaire sous contraite. Nous avons obtenu des champs de contrainte et de vitesse de déformation singuliers à l'extrêmité d'une fissure plane stationnaire, ce qui révèle le rôle de la cavitation sur le comportement du voisinage de l'extrémité de la fissure.

Zusammenfassung—Ausgehend von mikromechanischen Betrachtungen wird ein phänomenologisches Grundgesetz für das stationäre Kriechen eines polykristallinen Materials, in welchem sich kriechbedingt Hohlräume an Korngrenzen bilden, entwickelt. Singuläre Spannungsfelder und Felder der Verformungsgeschwindigkeit werden für die Spitze eines stationären ebenen Risses berechnet. Diese Felder weisen auf den Einfluß der Hohlraumbildung auf das Verhalten in der Nähe der Rißspitze hin.

INTRODUCTION

At high temperatures grain boundary cavitation is one of the primary mechanisms of deformation and failure in polycrystalline metals and ceramics. Recent work has served to clarify nucleation and growth processes associated with grain boundary voids [1, 2]. Second phase particles in the grain boundary interfere with sliding and nucleate voids early in the deformation history [3]. Whether these voids then grow or collapse depends on many factors including the temperature and local stress state at the boundary. If the voids do grow, they can do so by one of several mechanisms including diffusion [3], coupled diffusion and power-law creep [4] and power-law creep [5].

Only at high overall stresses will the growth mechanism predominately be due to power-law creep. This mechanism results in short lifetimes but extensive ductility, not unlike that associated with low temperature, time-independent void growth. In the range of low to moderate stresses, the lifetimes of high temperature alloys is long and the growth mechanism is predominately a diffusive one as evidenced by the low ductility which is usually observed. The voids grow and link up to form grain boundary cracks before extensive creep deformation of the grains can occur. An important feature of this process which has only recently been noted is that at sufficiently low overall stress the rate of void growth is constrained, or controlled, by the creep deformation of the grains, even though the local void growth mechanism is diffusive [6, 7]. The local stress driving diffusive growth of the many voids on a given grain boundary facet drops to a low level relative to the overall stress such that the net dilatation-rate of the voids is compatible with the slow creep distortion-rate of the surrounding grains. In other words, voiding along a facet cannot occur without an accommodating deformation of the surrounding grains. If these grains are deforming slowly enough, void growth has no difficulty keeping up and the rate of growth is determined by the creep of the grains. These notions are consistent with the experimental rule, known as the Monkman–Grant relation, for rupture life-times under constant stress loadings. It states that the time to failure for a polycrystalline metal at a given temperature varies roughly inversely with the steady-state, or minimum, creep-rate over the range of stress levels of practical interest. That is, the lifetime correlates with the overall creep behavior and not with the linear stress dependence expected from the diffusive process.

In this paper a multiaxial constitutive relation is proposed for steady-state creep of a polycrystalline material undergoing grain boundary cavitation. It will be assumed that the overall stresses are in the range such that the void growth is creep-constrained in the manner described above. Material constants characterizing diffusion do not appear explicitly in

this limiting creep-constrained condition. Following presentation of the constitutive law, we apply it to study the influence of cavitation in the stress and strain-rate fields at the tip of a macroscopic crack. Detailed results are presented for a stationary crack under conditions of plane strain and Mode I.

CONSTITUTIVE LAW FOR A POLYCRYSTALLINE MATERIAL UNDERGOING CREEP-CONSTRAINED GRAIN BOUNDARY CAVITATION

Attention is focused on the major portion of the lifetime of the polycrystal prior to the tertiary period when the cavitating facets start to link up leading to final rupture. The overall stress history is restricted to be proportional so that, in particular, the direction of the maximum principal stress does not change. It is assumed that only facets which are normal to (or nearly normal to) the maximum principal tensile stress direction suffer cavitation. This appears to be a reasonable assumption as evidenced by experimental observations of a number of investigators (e.g. [8, 9]). Furthermore, since the voids distributed over any such facet are assumed to have relaxed the traction acting across the facet to a low level relative to the overall stress, the net dilatation-rate from the facet can be estimated by modeling the facet as a traction-free micro-crack, as in the limiting case of creep-constraint considered in [7]. The macroscopic, or overall, steady creep-rate of the material is thus estimated from a model material which deforms according to power-law creep and which contains micro-cracks aligned normal to the maximum principal stress direction.

For such a material there exists a potential function of the overall stress, $\Phi(\sigma)$, such that the overall strain-rate is given by (see Appendix for background theory)

$$\dot{\epsilon}_{ij} = \frac{\partial \Phi}{\partial \sigma_{ij}}. \tag{1}$$

In the absence of micro-cracks the potential function is taken to be

$$\Phi_0 = \frac{\alpha \sigma_0}{n+1}\left(\frac{\sigma_e}{\sigma_0}\right)^{n+1} \tag{2}$$

where $\sigma_e = (3 s_{ij} s_{ij}/2)^{1/2}$ is the effective stress and $\mathbf{s}$ is the stress deviator. Via (1) this leads to the simple power-law relation for steady creep

$$\dot{\epsilon}_{ij} = \frac{3}{2}\alpha\left(\frac{\sigma_e}{\sigma_0}\right)^n \frac{s_{ij}}{\sigma_e} \quad \text{and} \quad \dot{\epsilon} = \alpha\left(\frac{\sigma}{\sigma_0}\right)^n \tag{3}$$

where the second relation holds in simple tension σ. Here α and σ_0 are a reference strain-rate and stress, respectively. It is assumed that the contribution from grain boundary sliding is included in equation (2), as analyzed for example in [10].

Each cavitating facet will be modeled as a penny-shaped micro-crack aligned normal to the direction of the maximum principal tensile stress S. An approximate analytic solution for an isolated penny-shaped crack in the power-law material (3) has been given in [11] for the case of general remote stress states which are axisymmetric with respect to the axis of the crack. With $\sigma_{11} = S$ and $\sigma_{22} = \sigma_{33} = T$ characterizing the remote stress state where x_1 is aligned with the axis of the crack, the rate of increase of the volume of the crack is given by [11]

$$\dot{V} = 8\alpha a^3\left(1+\frac{3}{n}\right)^{-1/2}\left(\frac{\sigma_e}{\sigma_0}\right)^n \frac{S}{\sigma_e} \tag{4}$$

where a is the radius of the crack and $\sigma_e = S - T$ when $S > T$. The ratio S/σ_e can be regarded as a measure of the triaxiality of the remote stress state. It equals unity for remote uniaxial tension perpendicular to the crack and is related to the ratio of remote mean stress, $\sigma_m = \sigma_{kk}/3$, to effective stress by

$$\frac{S}{\sigma_e} = \frac{\sigma_m}{\sigma_e} + \frac{2}{3}. \tag{5}$$

Highly accurate numerical calculations of $\dot{V}$ are presented in [11]. The analytical formula (4) was found to be accurate to within 1% for $S/\sigma_e \leq 2$ when $n \leq 5$, and it is exact when $n = 1$. For triaxialities above $S/\sigma_e = 3$, equation (4) underestimates $\dot{V}$ when $n > 1$. This can be seen in Fig. 1 where the ratio $\dot{V}(S,T)/\dot{V}(S,0)$ is plotted as a function of σ_e/S. Here, $\dot{V}(S,T)$ is the volume-rate for the crack subject to both S and T and $\dot{V}(S,0)$ denotes the rate under remote uniaxial tension S. The dashed curves are derived from (4) while the solid line curves are from the more accurate numerical results in [11]. Formula (4) incorrectly predicts $\dot{V} = 0$ for pure remote hydrostatic tension ($S = T$, $\sigma_e = 0$) when $n > 1$. However, as seen in Fig. 1, for loadings close to hydrostatic tension with $S \cong T$ so that $\sigma_e/S \ll 1$ the volume

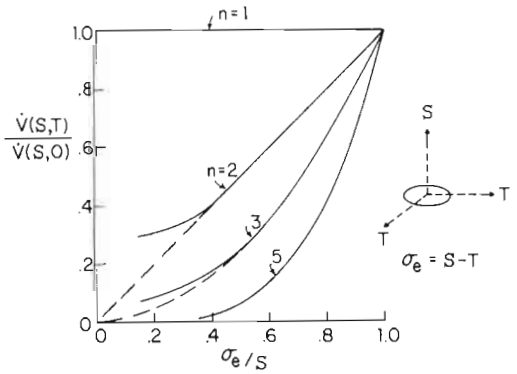

Fig. 1. Penny-shaped crack in an infinite block of power-law creeping material. Ratio of dilatation-rate under triaxial stressing ($\sigma_{11} = S$, $\sigma_{22} = \sigma_{33} = T$, with $S > T$) to that under uniaxial stressing ($\sigma_{11} = S$, $\sigma_{22} = \sigma_{33} = 0$). Solid line curves from accurate numerical results in [11]; dashed line curves from equation (4).

growth-rate is indeed much smaller than the corresponding rate for a crack subject to a uniaxial tension S when $n \geq 3$. Nevertheless, (4) will underestimate $\dot{V}$ at very high triaxialities, and the implication of this for the dilatation field at a macroscopic crack tip will be discussed later.

The potential function for the strain-rate contribution of an isolated penny-shaped crack in the power-law material is

$$\Phi_c = 4\alpha\sigma_0 a^3 \left(1+\frac{3}{n}\right)^{-1/2} \left(\frac{\sigma_e}{\sigma_0}\right)^{n+1} \left(\frac{S}{\sigma_e}\right)^2 \qquad (6)$$

where it is again understood that the axis of the crack lies along the direction of the maximum principal stress S. The strain-rate quantity $\partial\Phi_c/\partial\sigma_{ij}$ represents the contribution from a single, non-interacting crack to the overall strain-rate (see the Appendix for details). In particular, $\partial\Phi_c/\partial\sigma_m$ gives the volume-rate (4).

If the spacing between the cavitating facets (modeled as micro-cracks of radius a) is sufficiently great their interaction becomes unimportant. Then the total potential of the material with aligned micro-cracks is a superposition of equation (2) and contributions of the form (6). That is, the potential function can be written as

$$\Phi = \frac{\alpha\sigma_0}{n+1} \left(\frac{\sigma_e}{\sigma_0}\right)^{n+1} \left\{1+\rho\left(\frac{S}{\sigma_e}\right)^2\right\}. \qquad (7)$$

For widely spaced cavitating facets the factor ρ follows immediately from (6) as

$$\rho = 4a^3 N(n+1)(1+3/n)^{-1/2} \qquad (8)$$

where N is the number of cavitating facets per unit volume. However, we prefer to leave ρ as a free parameter whose role will be revealed below by the expression for the strain-rate. Using the connection $\dot{\epsilon}_{ij} = \partial\Phi/\partial\sigma_{ij}$, one finds

$$\dot{\epsilon}_{ij} = \alpha\left(\frac{\sigma_e}{\sigma_0}\right)^n \left\{\frac{3}{2}\frac{s_{ij}}{\sigma_e} + \rho\left[\frac{3(n-1)}{2(n+1)}\frac{s_{ij}}{\sigma_e}\left(\frac{S}{\sigma_e}\right)^2 + \frac{2}{n+1}\frac{S}{\sigma_e}m_{ij}\right]\right\} \qquad (9)$$

where m is the tensor whose components in the principal axes of stress are

$$m_{ij} = \delta_{iK}\delta_{jK} \quad \text{(no sum on } K\text{)} \qquad (10)$$

where δ_{ij} is the Kronecker delta and K denotes the index associated with the direction aligned with the maximum principal (tensile) stress S.

For uniaxial tension in the 1-direction with $\sigma_e = \sigma_{11} = S$, the strain-rate and dilatation-rate from equation (9) are

$$\dot{\epsilon}_{11} = \alpha\left(\frac{S}{\sigma_0}\right)^n (1+\rho) \quad \text{and} \quad \dot{\epsilon}_{kk} = \alpha\left(\frac{S}{\sigma_0}\right)^n \frac{2\rho}{n+1}. \qquad (11)$$

Thus, $\rho/(1+\rho)$ can be identified as the relative fraction of the tensile strain-rate due to grain-boundary cavitation in uniaxial tension. From (11)

$$\frac{\dot{\epsilon}_{kk}}{\dot{\epsilon}_{11}} = \frac{2}{n+1}\frac{\rho}{1+\rho} \qquad (12)$$

and, for example, ρ could be regarded as a parameter to be chosen to fit steady-state data according to equation (12) in the range of creep-constrained cavitation. Data in [8] for the cavitation-rate in uniaxial tension does indeed suggest a constant ratio of $\dot{\epsilon}_{kk}/\dot{\epsilon}_{11}$, and values of ρ on the order of unity result when equation (12) is used to fit that data. Values of ρ of this magnitude are consistent with a moderately low density of cavitating facets, although interaction between facets may make the dilute estimate (8) somewhat questionable. Even so, it can be hoped that the potential function (7) and the strain-rate expression (9) which derives from it have approximate validity when ρ is chosen to reproduce selected experimental data.

The form of the relation between strain-rate and stress given by equation (9) is quite different from the well-known phenomenological damage theory due to Kachanov (e.g. [12]). In that theory the damage parameter increases in time in accord with a prescribed equation, and under constant stress conditions the strain-rate increases with increasing damage. The description is inherently non-steady under constant stress. There is no provision in the Kachanov model for an overall dilatational contribution to the strain-rate, nor is there any effect on the strain-rate of the hydrostatic component of stress. The adequacy of the functional form of the Kachanov description as applied to creep-constrained cavitation has been questioned in [2] on the basis of micro-mechanical considerations similar to those discussed in the Introduction. Furthermore, experimental work (see [8]) has suggested that both a constant dilatation-rate and a hydrostatic stress dependence are associated with secondary, or steady, creep behavior under constant stressing in the regime of creep-constrained grain boundary cavitation.

In the present model ρ reflects the density of cavitating facets but not the microscopic damage *per se*. Thus, if the density of cavitating facets is fixed during some period of constant stressing, ρ will not change and the strain-rate will be steady even though microscopic damage is accumulating in the sense that the voids are enlarging. This behavior is a consequence of creep-constrained deformation and qualitatively, at least, is consistent with the notions discussed in [2, 7, 8]. The hydrostatic component of stress does affect the strain-rate. For example, if a hydrostatic tension p is superimposed on a uniaxial stress σ_e, the strain-rate from (9) is

$$\dot{\epsilon}_{11} = \alpha\left(\frac{\sigma_e}{\sigma_0}\right)^n \left\{1+\rho\left(1+\frac{p}{\sigma_e}\right)\left[1+\left(\frac{n-1}{n+1}\right)\frac{p}{\sigma_e}\right]\right\}. \qquad (13)$$

The contribution to the strain-rate from the cavitating facets in equation (9) includes a deviatoric part as well as a dilatant component. In fact, the deviatoric contribution is substantially larger than the dilatant component when the exponent n is 3 or more and $S/\sigma_e \geq 1$. For example, in simple tension the ratio of the dilatant to the uniaxial strain-rate contributions from the cavitating facets is $2/(n+1)$, and this ratio becomes even smaller under higher levels of triaxiality. The significance of the relatively large deviatoric contribution to the strain-rate will be brought out in the discussion of the crack tip fields.

The material characterized by equation (9) is an isotropic, power-law creeping solid. The strain-rate is a homogeneous function of degree n in the stresses. For $n = 1$, (9) reduces to

$$\dot{\epsilon}_{ij} = (\alpha/\sigma_0)\{\tfrac{3}{2}s_{ij} + \rho S m_{ij}\}. \tag{14}$$

While this relation is homogeneous of degree one, it is not linear in the stresses since neither S nor m_{ij} is a linear function of the stress components.

Finally, we emphasize that equations (4) and (6) were derived in [11] under conditions of axisymmetric stressing (i.e. $\sigma_{11} = S$ and $\sigma_{22} = \sigma_{33} = T$). Here we will assume that these formulas (and also (7) and (9) which follow from them) apply, at least approximately, under general stressing where the stresses are $\sigma_{11} = S$ with $\sigma_{22} \neq \sigma_{33}$ in principal axes, where S is again the maximum principal stress which is perpendicular to the micro-crack. For $n = 1$, equations (4) and (6) are exact, but for $n > 1$ the accuracy of these formulas has not been established for the more general stress conditions.

CRACK-TIP FIELDS FOR A MATERIAL UNDERGOING CREEP-CONSTRAINED GRAIN BOUNDARY CAVITATION

We consider a stationary macroscopic crack under steady creeping conditions. The crack is taken to lie along the negative x_1 axis and, for the moment, either plane stress or plane strain is assumed to prevail. The creep zone is asumed to be very large compared to the grain size and a continuum description of the material is employed based on equation (9). Under steady creep conditions the stresses at each point in the crack tip field do not vary with time. The orientation of the principal stress axes at any point also remains fixed. However the distribution of this orientation, and thus that of the cavitating facets, is not known in advance but is inherently an unknown element of the problem.

We will assume that in the region of concern near the crack tip the density of cavitating facets is approximately uniform so that ρ can be taken to be independent of position. (Of course, the *rate of cavitation* will be a strong function of position.) With constant ρ the material meets the conditions required for application of the C^*-integral to the macroscopic crack problem. This theory is simply the conversion to a steadily creeping material of J-integral theory for cracks in time-independent deformation theory materials. The line integral

$$C^* = \int_\Gamma (W n_1 - \sigma_{ij} n_j \dot{u}_{i,1}) \mathrm{d}s \tag{15}$$

is independent of path for all contours Γ encircling the crack tip such as that shown in Fig. 2. Here $\mathbf{n}$ is the outward unit normal to the contour, $\dot{\mathbf{u}}$ is the velocity, and

$$W = \int_0^{\dot{\epsilon}} \sigma_{ij}\, \mathrm{d}\dot{\epsilon}_{ij}. \tag{16}$$

For any power-law material W, Φ and the dissipation rate are related by

$$\sigma_{ij}\dot{\epsilon}_{ij} = \left(\frac{n+1}{n}\right) W = (n+1)\Phi \tag{17}$$

so that an expression for W in terms of the stresses follows immediately from equation (7).

The pure-power character of the constitutive law (9) permits a description of the crack-tip singularity fields in a separated form similar to the HRR-fields [13, 14]. With r and θ as planar polar coordinates centered at the crack tip, the fields have the form

$$\sigma_{ij} = \sigma_0 \left(\frac{C^*}{\alpha\sigma_0 I r}\right)^{1/(n+1)} \tilde{\sigma}_{ij}(\theta, n, \rho) \tag{18}$$

$$\dot{\epsilon}_{ij} = \alpha \left(\frac{C^*}{\alpha\sigma_0 I r}\right)^{n/(n+1)} \tilde{\dot{\epsilon}}_{ij}(\theta, n, \rho) \tag{19}$$

where $\tilde{\sigma}_{ij}$ and $\tilde{\dot{\epsilon}}_{ij}$ depend on the mode of loading and on whether plane strain or plane stress pertains, as does the normalizing factor $I \equiv I(n, \rho)$. The representation is made definite when the θ-variations are normalized in some manner. We will retain the normalization used in previous work [13] and require the maximum value of $\tilde{\sigma}_e$ to be unity for θ on the interval $(0, 2\pi)$. With the normalization in force, C^* plays the role of the amplitude of the singularity fields; it cannot be determined by the asymptotic near-tip analysis since it depends on the full geometry of the cracked body and on the external loading.

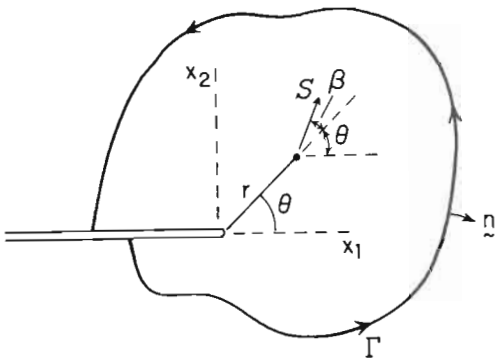

Fig. 2. Conventions for macroscopic crack analysis.

In the problem analyzed below the maximum principal stress lies in the (x_1, x_2)-plane and its distribution has the same form as equation (18), i.e.

$$S = \sigma_0 \left(\frac{C^*}{\alpha \sigma_0 I r} \right)^{1/(n+1)} \tilde{S}(\theta, n, \rho). \tag{20}$$

The angle which the maximum principal stress direction makes with the radial direction is denoted by $\beta(\theta, n, \rho)$ so that $\theta + \beta$ is the angle between the principal stress direction and the x_1-axis, as depicted in Fig. 2. By equation (9), the θ-variations of the strain-rates and stresses are related by

$$\dot{\tilde{\epsilon}}_{ij} = \tilde{\sigma}_e^n \left\{ \frac{3}{2} \frac{\tilde{s}_{ij}}{\tilde{\sigma}_e} + \rho \left[\frac{3(n-1)}{2(n+1)} \frac{\tilde{s}_{ij}}{\tilde{\sigma}_e} \left(\frac{\tilde{S}}{\tilde{\sigma}_e} \right)^2 + \frac{2}{n+1} \frac{\tilde{S}}{\tilde{\sigma}_e} m_{ij} \right] \right\} \tag{21}$$

Substitution of equations (18), (19) and a similar expression for $\dot{\mathbf{u}}$ into (15) gives the following expression for I in terms of the normalized θ-variations

$$I = \int_{\pi}^{\pi} \left\{ \frac{n}{n+1} \tilde{\sigma}_{ij} \dot{\tilde{\epsilon}}_{ij} - \tilde{\sigma}_{ij} n_j \dot{\tilde{u}}_{i,1} \right\} \mathrm{d}\theta. \tag{22}$$

With $\rho = 0$, the fields reduce to the incompressible HRR-fields. However, when $\rho \neq 0$ the cavitating facets make both deviatoric and dilatant contributions to the strain-rate, altering the entire crack tip field. For the remainder of this section we restrict attention to results for *Mode I cracks* under *plane strain* conditions ($\dot{\epsilon}_{33} = 0$). In plane strain it is readily shown that $s_{33} = 0$ and that the maximum principal stress S lies in the (x_1, x_2)-plane so that $m_{33} = 0$.

We will start by presenting the results for the limiting case in which $n = 1$. Polycrystalline creep with $n = 1$ is usually associated with a diffusive mode of deformation. In metals such a mode will generally only occur at extremely low stresses, but in ceramics such modes are usually the dominant ones even at relatively high stress. With $\rho = 0$ and $n = 1$, the solution is the classical (incompressible) linear elastic crack-tip field. The θ-variations of the stresses for this field are

$$\begin{Bmatrix} \tilde{\sigma}_{rr} \\ \tilde{\sigma}_{\theta\theta} \\ \tilde{\sigma}_{r\theta} \end{Bmatrix} = \frac{1}{2\sqrt{3}} \begin{Bmatrix} 5\cos\tfrac{1}{2}\theta - \cos\tfrac{3}{2}\theta \\ 3\cos\tfrac{1}{2}\theta + \cos\tfrac{3}{2}\theta \\ \sin\tfrac{1}{2}\theta + \sin\tfrac{3}{2}\theta \end{Bmatrix} \tag{23}$$

with $\tilde{\sigma}_{33} = (\tilde{\sigma}_{rr} + \tilde{\sigma}_{\theta\theta})/2$. For θ in the range $(0, \pi)$

$$\tilde{\sigma}_e = \sin\theta, \ \tilde{S} = \frac{1}{\sqrt{3}}(2\cos\tfrac{1}{2}\theta + \sin\theta) \quad \text{and} \quad \beta = \tfrac{1}{4}(\pi - \theta). \tag{24}$$

The maximum value of $\tilde{S}$ is 3/2 attained at $\theta = 60°$ with $\beta = 30°$, corresponding to the principal stress being directed in the x_2-direction. By contrast, ahead of the crack on $\theta = 0$, $\tilde{S} = 2/\sqrt{3}$ with $\beta = 45°$, which must be interpreted as a limiting condition for $\theta \to 0$ since $\sigma_{rr} = \sigma_{\theta\theta}$ with $\sigma_{r\theta} = 0$ on $\theta = 0$.

The field for $n = 1$ with $\rho > 0$ turns out to be exceptionally simple in that the θ-variations of the stresses are *independent of* ρ. The strain-rates derived from equation (19) and (21) with $\rho > 0$ in terms of the above θ-variations of the stresses in (23) and (24) satisfy compatibility. A transparent reason why this should be so has not been found; that it is true, however, has been established by direct substitution into the compatibility equation. Thus, equation (21) with (23) and (24) comprise the solution for all ρ when $n = 1$. Since $\tilde{\sigma}_{ij}$ are independent of ρ and since $\dot{\tilde{u}}_i$ and $\dot{\tilde{\epsilon}}_{ij}$ are linear in ρ, I in (22) must also be linear in ρ. We find

$$I = 2\pi + \left(\frac{4\pi}{3} + \frac{224}{45} \right) \rho = 6.28 + 9.17\rho \quad (\text{for } n = 1). \tag{25}$$

The distribution of the dilatation in the near-tip field from equations (19), (21) and (24) is

$$\dot{\epsilon}_{kk} = \frac{\alpha\rho}{\sqrt{3}} \left(\frac{C^*}{\alpha \sigma_0 I r} \right)^{1/2} (2\cos\tfrac{1}{2}\theta + \sin\theta), \ 0 \leq \theta \leq \pi. \tag{26}$$

At a given r-value, the maximum dilatation rate occurs at $\theta = 60°$.

Under certain circumstances, this simple solution may also have application to brittle elastic solids which undergo micro-cracking near the tip of a macroscopic crack. If the micro-cracks tend to align themselves normal to the maximum principal stress direction, then a time-dependent constitutive relation analogous to equation (14) should be applicable, although the assumption of a uniform density of such cracks may not be appropriate. Elastic compressibility in such a relation does not complicate the simplicity of the solution.

For $n > 1$ it is no longer true that the θ-variations of the stresses are independent of ρ. The numerical method used to solve for the θ-variations is similar to that used in the earlier analysis of the HRR-fields [13] and therefore it is unnecessary to repeat details of the method here.

The θ-variations of the stresses are shown in Fig. 3 for $n = 3$ and 5. The solid line curves are for $\rho = 0$ and these reproduce the corresponding HRR results in [13]. The dashed line curves were computed with $\rho = 1$ corresponding to a fairly substantial contribution from grain boundary cavitation, as discussed in connection with equation (11). Curves of $\tilde{S}$ and β are shown in Fig. 4 for the same sets of values of n and ρ. It can be seen that the θ-variations of the stresses are only weakly dependent on ρ. As in the case of $n = 1$, the main effect of ρ on the stresses arises through the normalizing factor I. Although I is not strictly linear in ρ when $n > 1$, we found that the numerical values for I could be well approximated by

$$I(n, \rho) = I_0(n) + \rho I_1(n) \tag{27}$$

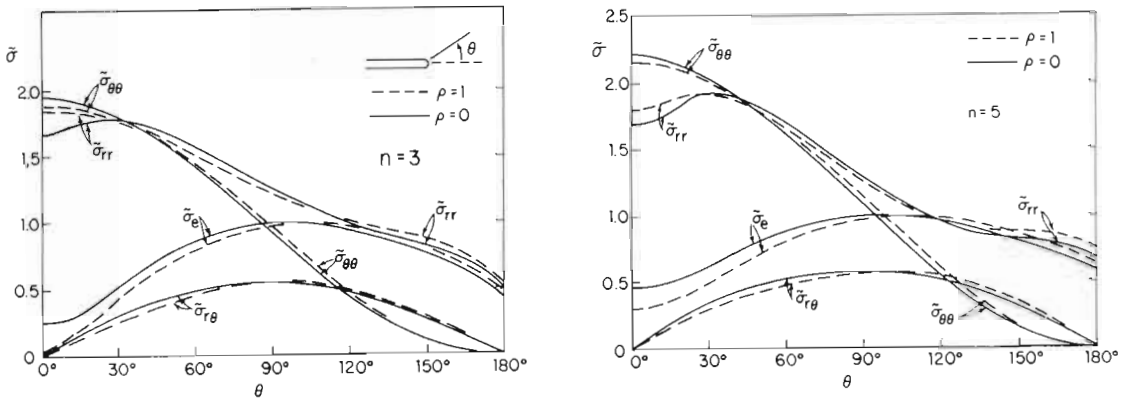

Fig. 3. θ-variations of the stress components of the singularity field.

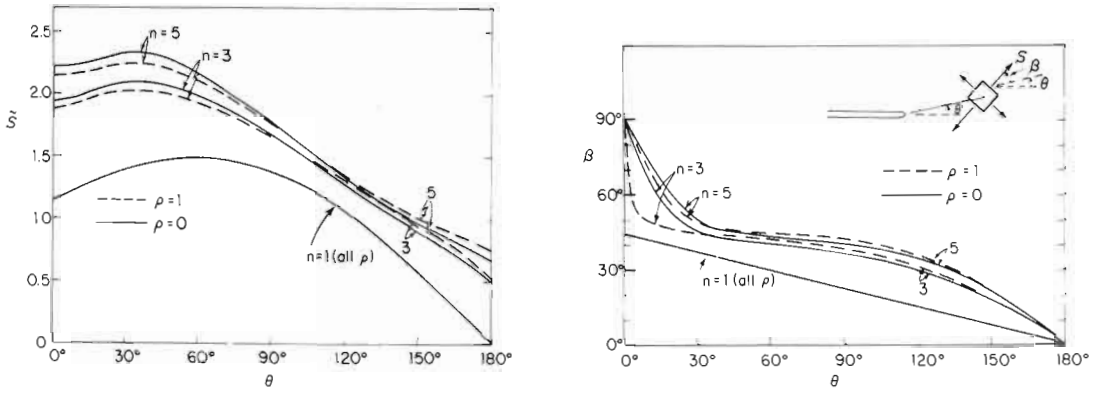

Fig. 4. θ-variations of the maximum principal stress of the singularity field together with its orientation.

where values of $I_0(n)$ and $I_1(n)$ are given in Table 1. The values for I_0 coincide with those of the HRR-field; the approximation (27) is accurate to within a few per cent for $\rho \leq 2$.

The θ-variations of the strain-rates are shown for $n = 3$ in Fig. 5 and for $n = 5$ in Fig. 6. These have been determined using equation (21) with the variations $\tilde{\sigma}_{ij}$ for the values of ρ shown. (We note, however, that a reasonable approximation for $\dot{\tilde{\epsilon}}_{ij}$ could be obtained using the HRR stress variations (corresponding to $\rho = 0$) in equation (21) since, as previously emphasized, the ρ-dependence of the $\tilde{\sigma}_{ij}$ is small.) Included in Figs 5 and 6 are the results for the θ-variations of the dilatation-rate, $\dot{\tilde{\epsilon}}_{kk}$, where from (19)

$$\dot{\epsilon}_{kk} = \alpha \left(\frac{C^*}{\alpha \sigma_0 I r} \right)^{n/(n+1)} \dot{\tilde{\epsilon}}_{kk} \tag{28}$$

and from (21)

$$\dot{\tilde{\epsilon}}_{kk} = \frac{2\rho}{n+1} \tilde{\sigma}_e^{n-1} \tilde{S}. \tag{29}$$

In the regime of creep-constrained cavitation being considered here, the cavitation rate is greatest where the creep-rate is greatest (i.e. where $\tilde{\sigma}_e$ is greatest) and this is reflected in the variation of $\dot{\tilde{\epsilon}}_{kk}$. Relatively little dilatation occurs directly ahead of the tip (except when $n = 1$), even though this is the region of high stress triaxiality, because the overall creep-rate is low there. As mentioned in the previous section, the present constitutive model underestimates the dilatation-rate in regions of high triaxiality when $n > 1$. The creep-rate is so low in the region of high triaxiality ahead of the crack that this inadequacy of the model is not expected to significantly affect the predictions.

Contours of constant dilatation-rate are shown in Fig. 7. In this figure a nondimensional, scaled polar coordinate $R(\theta)$ has been used where for a constant value of $\dot{\epsilon}_{kk}$

$$R = \left[\frac{(n+1)\dot{\epsilon}_{kk}}{2\alpha\rho} \right]^{(n+1)/n} \left(\frac{\alpha \sigma_0 I}{C^*} \right) r \tag{30}$$

Table 1. Values of I_0 and I_1

	I_0	I_1
$n = 1$	6.28	9.17
$n = 3$	5.51	13.3
$n = 5$	5.01	12.4

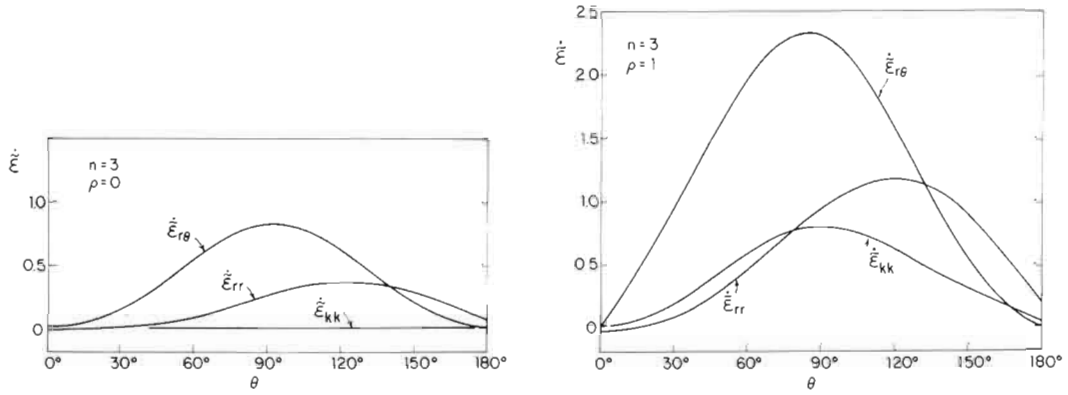

Fig. 5. θ-variations of the strain-rate components of the singularity field for $n = 3$ with $\rho = 0$ and 1.

so that, from equations (28) and (29), $R(\theta) = (\tilde{\sigma}_e^{n-1}\tilde{S})^{(n+1)/n}$. This scaling provides all contours of constant dilatation-rate in the zone dominated by the singularity fields. It can be noted that $R(\theta)$ is only weakly dependent on ρ for $n = 3$ and 5, while it is independent of ρ for $n = 1$.

It is also revealing to examine the distribution of the dissipation-rate near the crack tip. From equations (18), (19) and (21),

$$\sigma_{ij}\dot{\epsilon}_{ij} = \frac{C^*}{r}\tilde{D}(\theta, n, \rho) \tag{31}$$

where

$$\tilde{D} \equiv \tilde{\sigma}_{ij}\dot{\tilde{\epsilon}}_{ij}/I = \tilde{\sigma}_e^{n+1}[1 + \rho(\tilde{S}/\tilde{\sigma}_e)^2]/I. \tag{32}$$

Plots of $\tilde{D}$ as a function of θ are shown in Fig. 8 where it is seen that $\tilde{D}$ is only weakly dependent on both n and ρ, with the strongest dependence showing up in the limit $n = 1$. The distribution of dissipation near a crack tip at a given C^*-level is therefore relatively insensitive to whether or not cavitation is taking place and to the material parameters in general.

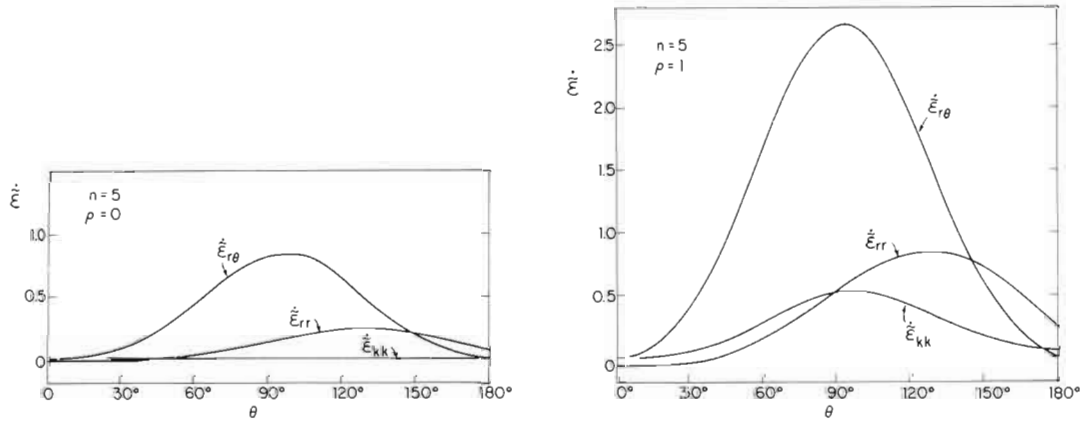

Fig. 6. θ-variations of the strain-rate components of the singularity field for $n = 5$ with $\rho = 0$ and 1.

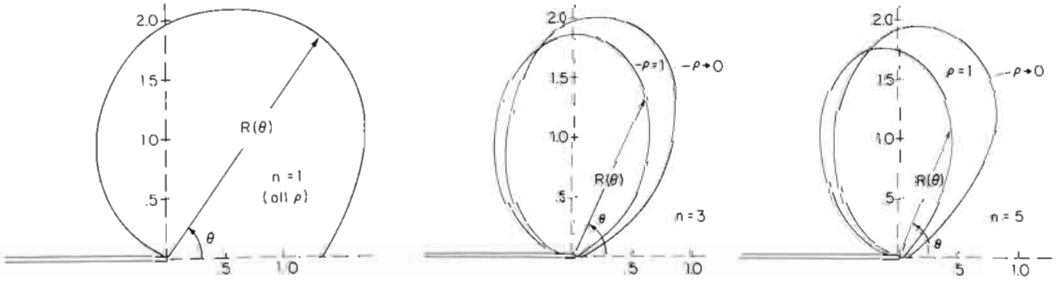

Fig. 7. Contours of constant dilatation-rate in the singularity field. The scaled, nondimensional variable $R(\theta)$ is defined in equation (30).

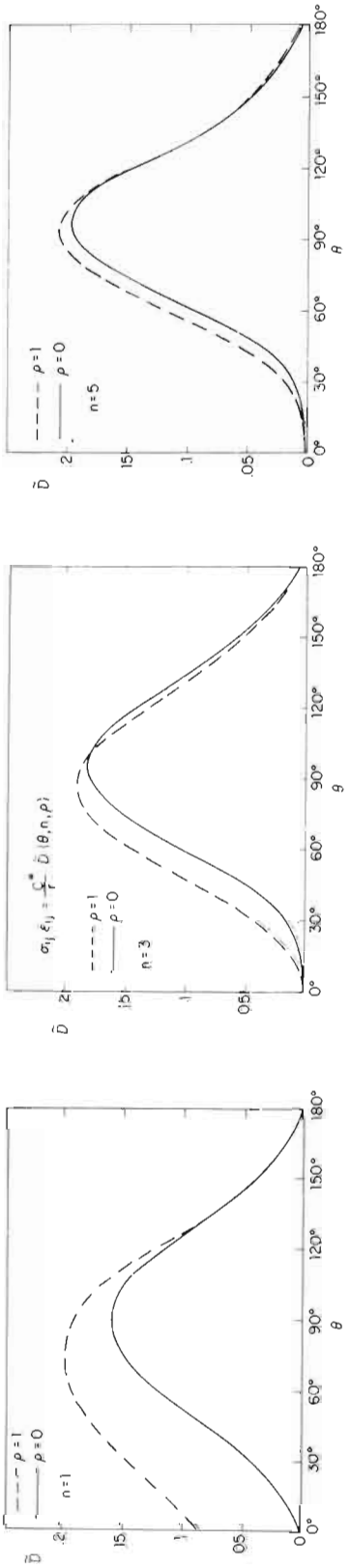

Fig. 8. θ-variations of the dissipation-rate in the singularity field.

CONCLUDING REMARKS

The asymptotic analysis of the crack tip fields has been idealized in several respects including the assumptions (i) that creep-constrained grain boundary cavitation pertains, (ii) that the density of cavitating facets is uniform near the tip, and (iii) that transient, or nonsteady, deformation can be ignored. In addition, attention has been restricted to a stationary macroscopic crack. In spite of these limitations, certain features revealed by the results are likely to remain unchanged by further refinements. In particular, for $n \geq 3$, the distribution of stresses and strain-rates near the tip remain relatively unchanged by the occurrence of cavitation, except that (for a given C^*-level) the stress level drops and the strain-rate level increases such that essentially the same distribution of the dissipation-rate is maintained. It is to be expected that there will be a fall off in the density of cavitating facets with distance from the tip, and far enough from the tip it is likely that essentially no voids will be nucleated. Under these circumstances, it is of course not true that the line integral (15) defining C^* remains path-independent. But, C^* as used in equations (18) and (19) may still retain its role as the amplitude of the near-tip fields if it is defined by the line integral using a near-tip contour. It is possible that the "far field" value of the line integral may not be too different from its near-tip value. (This would be consistent with the observation that the distribution of the dissipation-rate does not appear to be much influenced by the level of cavitation.) If so, analyses which ignore the effects of cavitation may be used to estimate the near-tip C^*, but this can only be ascertained by additional numerical studies.

The steady-state analysis carried out here ignores any elastic accommodation of grain boundary cavitation which is likely to occur in the early transient response of the material. Since the stresses ahead of the crack tip start out relatively high and then relax to lower values, it is possible that significant cavitation on facets directly ahead of the tip may occur before steady-state conditions are achieved. Nevertheless, the cavitation-rate on such facets should be much reduced as steady conditions are approached if, indeed, creep-constrained cavitation pertains.

Finally, the present results can be used to gain some insight into damage calculations such as those in [15, 16] which use stress distributions determined without accounting for the effects of cavitation to estimate void accumulation near a crack tip. For example, suppose one used the stresses from the HRR-fields (the present solution with $\rho = 0$) to estimate the dilatation-rate for a material with nonzero ρ obeying the constitutive law equation (9). Substitution of the HRR-stresses into (9) and evaluation of $\dot{\epsilon}_{kk}$ gives precisely the form of the correct result (28) but with I replaced by I_0 and with $\tilde{\sigma}_e$ and $\tilde{S}$ of the HRR-field in equation (29). The θ-variations of the HRR-stresses are not significantly different than

those for nonzero ρ, as has already been discussed. However, I is a strong function of ρ, and its replacement by I_0 means that the approximate calculation substantially overestimates the dilatation-rate at any given point. For $n = 3$ and $\rho = 1$, the approximate dilatation-rate is high by a factor of three. As emphasized in the discussion of the constitutive law, this is not so much a consequence of the dilatation, *per se*, but is due to the relatively large deviatoric strain-rate contribution from the cavitating facets and its effect on lowering the stress level near the tip.

Acknowledgements—This work was supported in part by the National Science Foundation under Grants CME-78-10756 and DMR-80-20247, and by the Division of Applied Sciences, Harvard University.

REFERENCES

1. A. S. Argon, I. W. Chen, C. W. Lau, in *Creep-Fatigue-Environment Interactions* (edited by R. M. Pelloux and N. S. Stoloff), p. 46. A.I.M.E., Warrendale, PA (1980).
2. A. C. F. Cocks and M. F. Ashby, *Prog. Mater. Sci.* **27,** 189 (1982).
3. T.-J. Chuang, K. I. Kagawa, J. R. Rice and L. Sills, *Acta metall.* **27,** 265 (1979).
4. A. Needleman and J. R. Rice, *Acta metall.* **28,** 1315 (1980).
5. B. Budiansky, J. W. Hutchinson and S. Slutsky, in *Mechanics of Solids, The Rodney Hill 60th Anniversary Volume* (edited by H. G. Hopkins and M. J. Sewell). p. 13. Pergamon Press, Oxford (1982).
6. B. F. Dyson, *Metals Sci.* **10,** 349 (1976).
7. J. R. Rice, *Acta metall.* **29,** 675 (1981).
8. B. F. Dyson, A. K. Verma and Z. C. Szkopiak, *Acta metall.* **29,** 1573 (1981).
9. W. A. Trampezynski, D. R. Hayhurst and F. A. Leckie, *J. Mech. Phys. Solids* **29,** 353 (1981).
10. F. Ghahremani, *Int. J. Solids Struct.* **16,** 847 (1980).
11. M. Y. He and J. W. Hutchinson, *J. appl. Mech.* **48,** 830 (1981).
12. F. A. Leckie and D. R. Hayhurst, *Acta metall.* **25,** 1059 (1977).
13. J. W. Hutchinson, *J. Mech. Phys. Solids* **16,** 13 and 337 (1968).
14. J. R. Rice and G. Rosengren, *J. Mech. Phys. Solids* **16,** 1 (1968).
15. H. Riedel, in *Creep in Structures* (edited by A. R. S. Ponter and D. R. Hayhurst). Springer, Berlin (1981).
16. J. L. Bassani and V. Vitek, *Proc. 9th U.S. National Congr. Applied Mechanics*, Cornell University (1982). To be published.

APPENDIX

Macroscopic behavior of a steadily creeping body with micro-cracks

As a representative macroscopic volume element, consider a body with many traction-free micro-cracks, whose orientations are for the moment assumed to be fixed independently of the overall stress. The body is assumed to be deforming under steady-state creep conditions. In this Appendix τ and $\dot{\eta}$ will denote local stress and strain-rate while σ and $\dot{\epsilon}$ will continue to signify overall, or macroscopic, stress and strain-rate. The steady creep law characterizing the material is specified by potential functions w and ϕ of the local strain-rate and stress, respectively, such that

$$\tau_{ij} = \partial w/\partial \dot{\eta}_{ij} \quad \text{and} \quad \dot{\eta}_{ij} = \partial \phi/\partial \tau_{ij} \tag{A1}$$

with

$$\tau_{ij}\dot{\eta}_{ij} = w + \phi. \tag{A2}$$

The volume of the macroscopic volume element is V and its outer surface is denoted by A. Following a standard approach in the theory of heterogeneous materials, let "uniform tractions" $\sigma_{ij}n_j$ be prescribed over A where n is the outward unit normal to A and σ_{ij} is independent of position. Define the overall strain-rate resulting from these tractions as

$$\dot{\epsilon}_{ij} = V^{-1}\int_A \frac{1}{2}(\dot{u}_i n_j + \dot{u}_j n_i)\,\mathrm{d}A \tag{A3}$$

where $\dot{u}$ is the local displacement-rate. Next note that

$$\dot{\epsilon}_{ij}\mathrm{d}\sigma_{ij} = V^{-1}\int_A \dot{u}_i n_j \mathrm{d}\sigma_{ij}\mathrm{d}A = V^{-1}\int_A \dot{u}_i n_j \mathrm{d}\tau_{ij}\mathrm{d}A$$
$$= V^{-1}\int_V \dot{\eta}_{ij}\mathrm{d}\tau_{ij}\mathrm{d}V = V^{-1}\int_V \mathrm{d}\phi\,\mathrm{d}V \tag{A4}$$

where use has been made of the traction condition, $\tau_{ij}n_j = \sigma_{ij}n_j$, on A, the principal of virtual work, and the condition that the micro-cracks are traction-free. It follows from (A4) that the macroscopic potential function

$$\Phi(\sigma) = V^{-1}\int_V \phi\,\mathrm{d}V$$

provides the overall strain rate according to

$$\dot{\epsilon}_{ij} = \partial\Phi/\partial\sigma_{ij}. \tag{A5}$$

A dissipation functional of the displacement-rate for the body with prescribed tractions $\sigma_{ij}n_j$ on A is defined in analogy with the potential energy functional for an elastic solid as

$$P = \int_V w\,\mathrm{d}V - \int_A \sigma_{ij}n_j\dot{u}_i\mathrm{d}A. \tag{A6}$$

From the fact that the actual fields in the body satisfy

$$\int_A \sigma_{ij}n_j\dot{u}_i\mathrm{d}A = \int_V \tau_{ij}\dot{\eta}_{ij}\mathrm{d}V$$

and the connection (A2), it follows that

$$P = -V\Phi(\sigma) \tag{A7}$$

when evaluated in terms of the solution for the micro-cracked volume element.

Now it is imagined that all the micro-cracks are penny-shaped cracks of radius a so that under constant σ, from (A7),

$$\frac{\mathrm{d}P}{\mathrm{d}a} = -V\frac{\mathrm{d}\Phi}{\mathrm{d}a}. \tag{A8}$$

When the micro-cracks are sufficiently far apart, $\mathrm{d}P/\mathrm{d}a$ can be estimated using results for an isolated crack in an infinite body under remote stress σ. Based on a penny-shaped crack in an infinite block of power-law material (2), the estimate of $\mathrm{d}P/\mathrm{d}a$ from [11] is

$$\frac{\mathrm{d}P}{\mathrm{d}a} = -12NV\alpha\sigma_0 a^2\left(1+\frac{3}{n}\right)^{-1/2}\left(\frac{\sigma_e}{\sigma_0}\right)^{n+1}\left(\frac{S}{\sigma_e}\right)^2 \tag{A9}$$

where N is the number of cracks per unit volume. Now the cracks are all assumed to be aligned normal to the direction of the maximum principal stress S, as discussed in the body of the paper. Integrating (A8) with respect to a using (A9) and noting that Φ is given by (2) when $a = 0$, we obtain Φ as given by (7) along with (8).

It is only intended that the constitutive relation be applied under conditions in which the direction of the maximum principal stress does not change so that the orientation of the cavitating facets remains fixed. Under this restriction on the stresses, it is readily shown that $\dot{\epsilon}_{ij} = \partial\Phi/\partial\sigma_{ij}$ leads to the strain-rate expression (9). However, we further note that this same strain-rate expression is also obtained from $\dot{\epsilon}_{ij} = \partial\Phi/\partial\sigma_{ij}$ when no restriction is placed on the stresses. Consequently, the restriction to stress histories with fixed (or nearly fixed) maximum principal stress direction is based on physical, but not mathematical, considerations.